

# 1 Higgs boson experimental overview for ICHEP 2020

---

2 **Christopher Palmer on behalf of the ATLAS and CMS Collaborations<sup>a,\*</sup>**

3 <sup>a</sup>*Princeton University*

4 *Princeton, NJ 08544*

5 *United States*

6 *E-mail: [cp10@princeton.edu](mailto:cp10@princeton.edu)*

7 Measurements of the kinematic properties of the Higgs boson with proton–proton collision data at  $\sqrt{s} = 13$  TeV collected by the ATLAS and CMS detectors at the Large Hadron Collider (LHC) during Run 2 (2015-2018) are summarized. Many measurements are reported with full LHC Run 2 luminosity of approximately  $140 \text{ fb}^{-1}$  – including the Higgs boson to two photons channel from both experiments. The Higgs boson to two photon analyses in both experiments make measurements in fine kinematic bins in all main production mechanisms. In addition, the first evidence of the Higgs boson decaying to two muons in CMS is described. A contemporary, precision-breaking combination of Higgs boson searches from ATLAS is also shown.

*40th International Conference on High Energy physics - ICHEP2020  
July 28 - August 6, 2020  
Prague, Czech Republic (virtual meeting)*

---

\*Speaker

## 1. Introduction

In 2012, the Higgs boson with mass of about 125 GeV was first observed independently by the ATLAS [1] and CMS [2] collaborations using only a portion of the Large Hadron Collider's (LHC) Run 1 data set of proton-proton collisions collected at  $\sqrt{s} = 7$  and 8 TeV [3, 4]. LHC's Run 2 proton-proton collisions at  $\sqrt{s} = 13$  TeV provided by ATLAS and CMS collaborations with an opportunity to characterize this Higgs boson with very large data sets. In total, the LHC provided approximately  $140 \text{ fb}^{-1}$  to each experiment. Taking into account the increase in production cross-section and increase in analyzed luminosity, there are roughly a factor 35 more Higgs bosons than in the discovery data sets and roughly a factor 13 more than in the full Run 1 data set.

As many analyses are completed with the full Run 2 data set, the Higgs boson observed couplings and production cross sections are highly compatible with the Standard Model (SM). The mature channels, such as two photon (Section 2), four lepton and two tau (Section 5), are abundant enough to allow ATLAS and CMS to measure production cross sections in fine bins of Higgs boson kinematic variables and probe Beyond the Standard Model (BSM) couplings (i.e., CP-violating and anomalous couplings). Moreover, the first second-generation fermion coupling has come into view with the evidence of the Higgs boson decaying to a pair of muons from CMS (Section 6), which utilizes a novel procedure in the category targeting the VBF production mode. Finally, a combination of many full Run 2 channels by the ATLAS collaboration gives the most finely-binned characterization of the Higgs boson to date in the Simplified Template Cross-Sections (STXS) framework [5–7].

## 2. Full Run 2 data set analysis of Higgs boson decays to two photons

Both the ATLAS and CMS collaborations released their full Run 2 results and measurements in the Higgs boson di-photon decay channel [8, 9]. Both analyses center on high-resolution di-photon events, which are triggered. Both analyses use hadronic jets (including those specifically arising from bottom quarks), electrons, muons and missing transverse momentum to tag non-gluon fusion (ggH) production channels (i.e., VBF, VH, ttH, and tH). CMS make direct selections on these quantities, and if no additional production mode tag selection is satisfied, the events are analyzed as ggH-produced Higgs boson candidates.

For ggH analyzed events in CMS and all di-photon events in ATLAS Boosted Decision Tree (BDT) multiclassifiers are used to predict the most likely STXS kinematic bin for each event. Both BDTs take photon and di-photon kinematic variables as well as information about other high transverse momentum hadronic jets, whereas much more information is included in ATLAS for the production mode classification. The output is a unity-normalized vector with length of the number of STXS bins targeted. The highest value index can be interpreted as the most likely STXS bin. The ATLAS BDT outputs are further weighted prior to assignment using pseudodata to minimize the covariance of measured STXS signal strengths. Figure 1 shows an example of one of the weighted outputs in ATLAS's multiclassifier, as well as, the validation of CMS's ggH multiclassifier using Z boson to electron pair events where electrons are treated like photons.

After the most likely STXS class is selected, both analyses use binary background-rejection BDTs to optimize background discrimination in each class. After discarding some events based

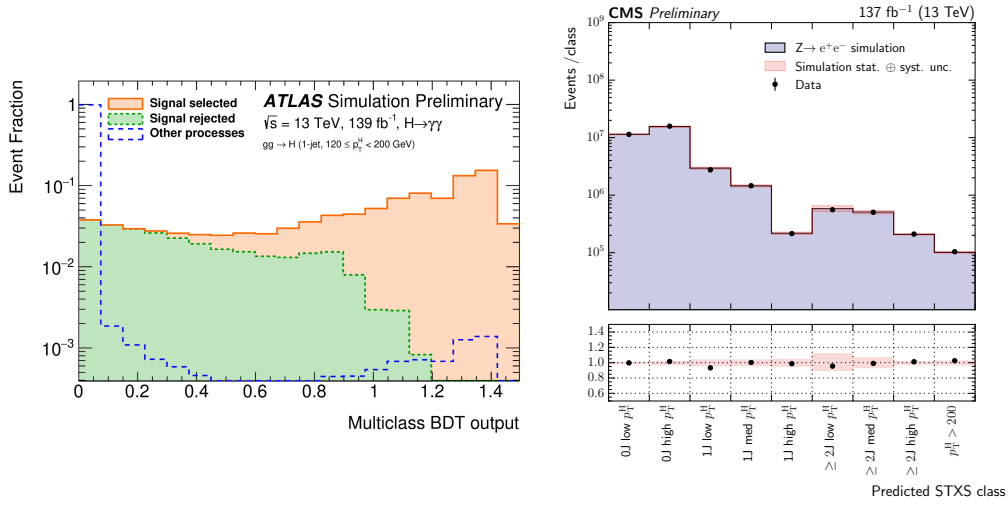


**Figure 1:** The left figure shows the weighted multiclassifier output for one STXS bin [9]. The right figure shows the predicted STXS class in data and MC using Z boson events and treating electrons like photons [8].

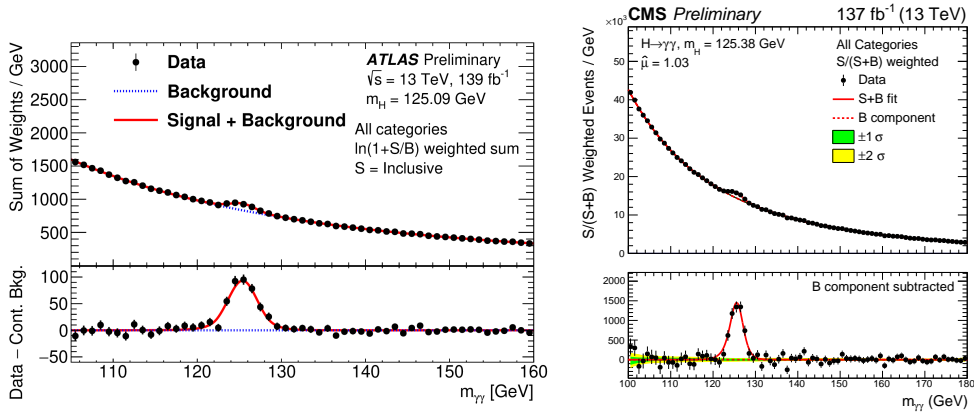


**Figure 2:** The di-photon invariant mass distributions for the weighted combination of all event categories ATLAS on the left [9] and CMS on the right [8]. The lower panel shows the residuals after background subtraction, with the best-fit SM Higgs boson signal contribution with  $m_H = 125.38$  (CMS) and 125.09 (ATLAS) GeV indicated by the red lines.

48 on a cut in the second BDTs, further classification is performed using these BDTs in many cases.  
 49 Finally, the invariant mass is graphed and fit in all the categories to extract the STXS signal strengths.  
 50 Figure 2 shows the combined mass plots from the two experiments. Although 44 (43) STXS bins  
 51 are considered by ATLAS (CMS), not all bins are accessible and many are merged with adjacent  
 52 bins. Figure 3 shows the 17-bin STXS results for CMS. CMS has an alternative result with 24  
 53 STXS bins and the analogous ATLAS result contains an impressive 27 STXS bins.

### 54 3. Observation of VBF Higgs boson to WW in ATLAS

55 ATLAS observed the VBF production of Higgs bosons in the  $WW \rightarrow e\nu\mu\nu$  decay channel with  
 56 the full Run 2 data set [10]. The signal is observed (expected) with a significance of  $7.0\sigma$  ( $6.2\sigma$ ).

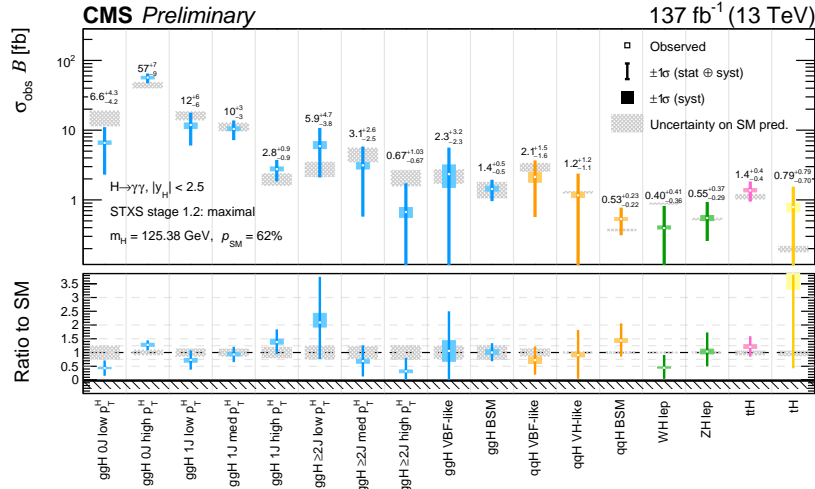


**Figure 3:** The 17-bin STXS results for the CMS Higgs boson to di-photon analysis [8].

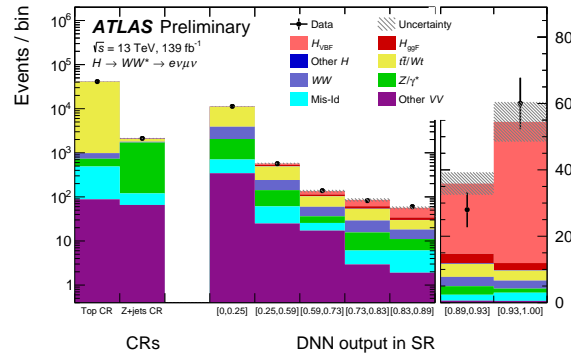


**Figure 4:** Post-fit distribution of the DNN output in the VBF signal region, together with the top and Z+jets control regions. The hatched band shows the total uncertainty of the signal and background modelled contributions [10].

57 Control regions (CRs) are used to normalize backgrounds with top quarks and Z bosons. The VBF  
 58 signal is extracted using a DNN discriminator. Figure 4 shows the CRs and signal discriminator.  
 59 The product of the total VBF cross-section times the  $WW^*$  branching fraction is measured to be  
 60  $0.85 \pm 0.10(\text{stat})_{-0.13}^{+0.17}(\text{syst})\text{pb}$ , compatible with the SM prediction of  $0.81 \pm 0.02\text{pb}$ .

#### 61 4. Strong evidence of Higgs boson production with top quarks with leptons in CMS

62 CMS completed the Higgs boson production rate in association with either one (tH) or two  
 63 (ttH) top quarks by tagging final states containing multiple electrons, muons, or tau leptons decaying  
 64 to hadrons and a neutrino using the full Run 2 data set. The analysis is aimed at events where Higgs  
 65 bosons have decayed to W bosons, Z bosons or tau leptons and each of the top quark(s) decays either  
 66 to lepton+jets or all-jet channels. Sensitivity to signal is maximized by including ten signatures  
 67 in the analysis, depending on the lepton multiplicity. The separation among the tH, the ttH, and

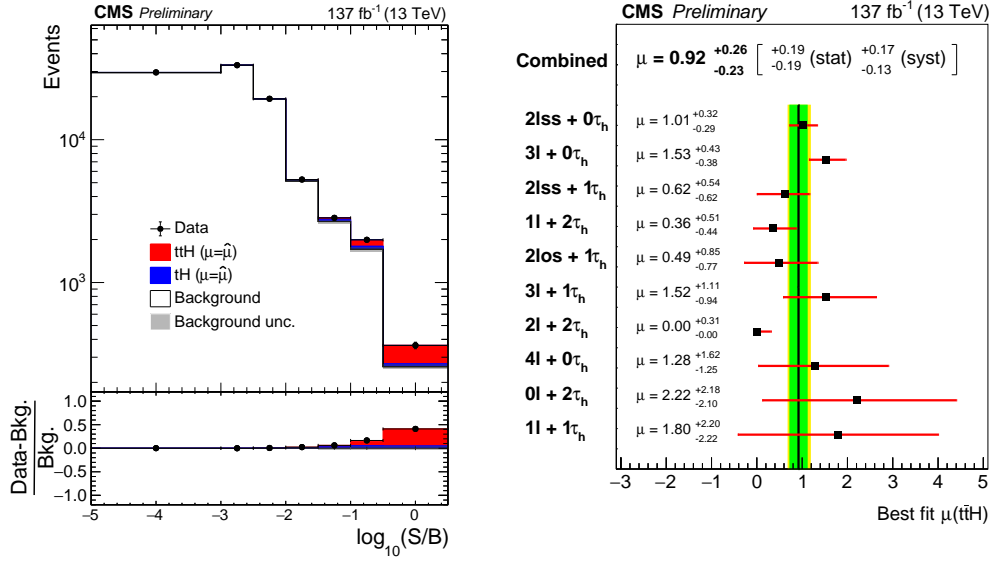


**Figure 5:** The left figure shows the combined distribution of the decimal logarithm of the ratio between the expected ttH+tH signal and the expected sum of background contributions in each bin of the 105 distributions that are included in the ML fit used for the signal extraction. The right figure shows the production rate of ttH signals, in units of their rate of production expected in the SM, measured in each of the ten channels individually and for the combination of all channels. The central value of the signal strength in the  $2\ell + 2\tau_h$  is constrained to be greater than zero. [11].

68 the backgrounds is enhanced through machine-learning discriminants and matrix-element methods.  
 69 Figure 5 shows all the discriminants combined in data and MC based on the value of the log(S/B)  
 70 in the bins of the observables as well as the signal strength in all ten signatures overlaid with the  
 71 best single signal strength. The measured production rates for the ttH and tH signals correspond  
 72 to  $0.92 \pm 0.19(\text{stat})_{-0.13}^{+0.17}(\text{syst})$  and  $5.7 \pm 2.7(\text{stat}) \pm 3.0(\text{syst})$  of their respective SM expectations.  
 73 The corresponding observed (expected) significance amounts to 4.7 (5.2) standard deviations for  
 74 ttH, and to 1.4 (0.3) for tH production.

## 75 5. BSM coupling constraints using Higgs boson events

76 The Higgs to two Z bosons to four-lepton (i.e., electrons or muons) channel offers an extremely  
 77 low-background sample of Higgs boson. The final state kinematic distributions (e.g., opening angles  
 78 between lepton pairs and the two Z bosons) contain the imprint of Higgs couplings, as well as the  
 79 Higgs boson quantum numbers. The CMS full Run 2 analysis uses a matrix element likelihood  
 80 approach (MELA) to discriminate first from background processes with cuts and then several  
 81 MELA outputs with sensitivity to the targeted couplings are used as observables [12]. Results are  
 82 interpreted in two (mapable) frameworks: anomalous couplings and effective field theory. Figure 6  
 83 shows the results for coupling strengths of the Higgs boson with gluons.

84 The Higgs to two tau lepton final state with full Run 2 data has been completed by CMS [13].  
 85 The fitted signal strength is  $0.85_{-0.11}^{+0.12}$  and 11 STXS bins in the ggH and VBF production modes are  
 86 measured. With this large data set, estimates of CP-violation can be made using opening angles

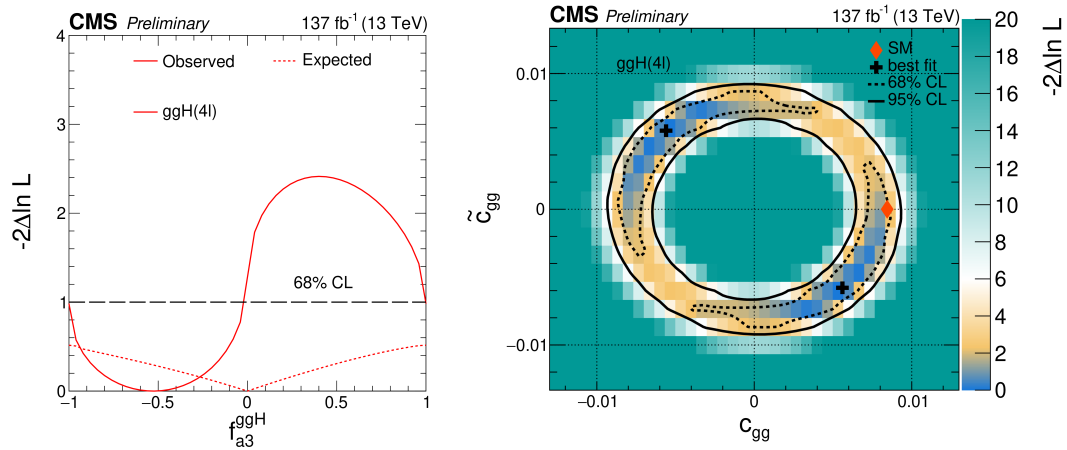


**Figure 6:** Constraints on anomalous Higgs boson couplings to gluons using the Higgs boson to four-lepton decay. Left: Observed (solid) and expected (dashed) likelihood scans of the CP-sensitive parameter  $f_{a3}^{ggH}$ . The dashed horizontal lines show 68% and 95% CL. Right: Observed confidence level intervals on the  $c_{gg}$  and  $\tilde{c}_{gg}$  couplings reinterpreted from the  $f_{a3}^{ggH}$  and  $ggH$  production strength measurement with  $f_{a3}$  and  $\mu_V$  profiled [12].

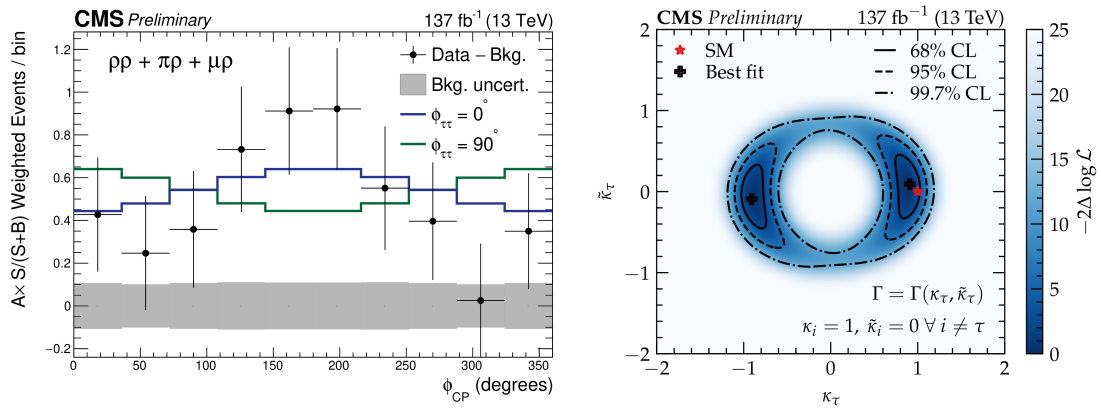


**Figure 7:** On the left there is the  $\phi_{CP}$  distribution for the three most sensitive channels combined. Events were collected from all years and NN/BDT bins in the three signal categories. The background is subtracted from the data. The events are reweighed via  $A \times S/(S+B)$ , in which  $S$  and  $B$  are the signal and background rates, respectively, and  $A$  is a measure for the average asymmetry between the scalar and pseudoscalar distributions. On the right there is the two-dimensional scan of the (reduced) CP-even ( $\kappa$ ) and CP-odd ( $\tilde{\kappa}$ )  $\tau$  Yukawa couplings [14].

87 between decay products. This measurement is optimized with machine learning discriminators [14].

88 Figure 7 summarizes the results showing data with background subtraction and a two-dimensional

89 scan of the CP-even (SM) and CP-odd parameters.

## 90 6. Evidence for Higgs boson decays to di-muon pairs

91 One of the most significant results from this conference—and possibly from LHC Run 2—is the

92 evidence for the Higgs boson decaying to two muons. This is the first evidence of any second-

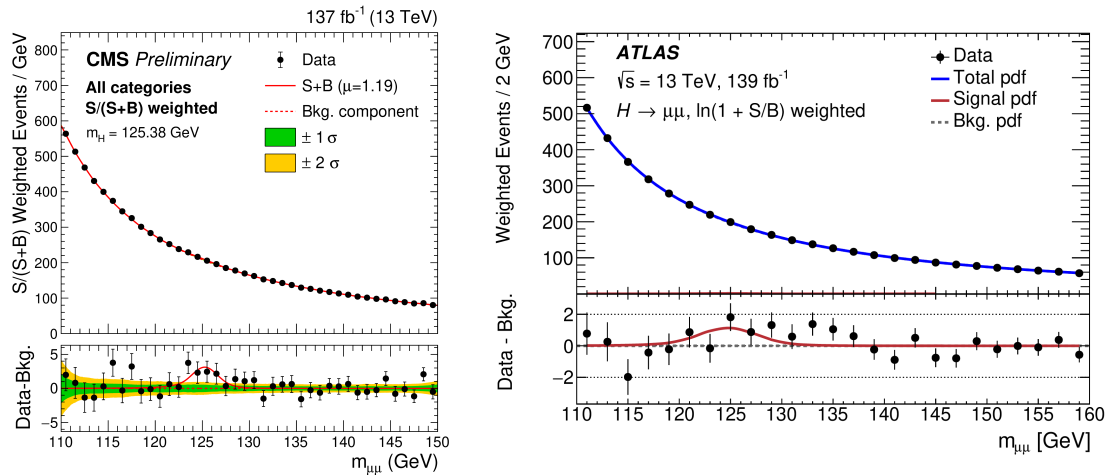


**Figure 8:** The di-muon invariant mass distributions for the weighted combination of all event categories CMS on the left [15] and ATLAS on the right [16]. The upper panel is dominated by the ggH categories with many data events but relatively small weight. The lower panel shows the residuals after background subtraction, with the best-fit SM Higgs boson signal contribution with  $m_H = 125.38$  (CMS) and 125.09 (ATLAS) GeV indicated by the red lines.

93 generation fermion coupling with the Higgs boson. All measurements are SM-compatible.

94 In the analyses from both the ATLAS and CMS collaborations the analysis centers on the  
 95 selection of two opposite-sign muons with invariant mass of at least 110 GeV [15, 16]. After that  
 96 various additional objects are sought for further categorization targeting the main production modes  
 97 (i.e., ggH, VBF, VH and ttH) of the Higgs boson at the LHC. In both analyses the invariant mass  
 98 spectra in all categories (with one exception) are fit simultaneously to extract the background shape  
 99 in each and the overall signal strength. The combined, weighted invariant mass plots with fitted  
 100 signal strength for ATLAS and CMS are shown in Figure 8.

101 The VBF di-jet tagged category from CMS has two novel features compared to all other  
 102 categories in CMS and ATLAS: 1) the observable is the output of a deep neural network (DNN) and  
 103 2) Monte Carlo (MC) templates are used to model the backgrounds. Selection targeting the di-jet  
 104 signature of two, high-energy, well-separated jets is required on top of the high quality di-muon  
 105 pair. The signal region (SR) requires a di-muon mass of 115-135 GeV. The sideband region (SB)  
 106 requires a mass of 110-150 or 135-150 GeV. The SR DNN uses the di-muon mass as input, whereas  
 107 the SB DNN is mass de-correlated. The SR and SB regions fit together to determine the primary  
 108 backgrounds' normalizations and shapes, while simultaneously extracting the signal. They are  
 109 shown in Figure 9.

110 The CMS analysis reports the first evidence for the decay of Higgs bosons to di-muons with  
 111 observed (expected) significance of  $3.0\sigma$  ( $2.5\sigma$ ) at CMS's most precisely measured Higgs boson  
 112 mass of 125.38 GeV. The observed signal strength is  $1.19^{+0.44}_{-0.42}$ . ATLAS reports an observed  
 113 (expected) significance of  $2.0\sigma$  ( $1.7\sigma$ ) at a Higgs boson mass of 125.09 GeV with a signal strength  
 114 of  $1.2 \pm 0.6$ . Figure 10 shows the CMS p-value scan over hypothetical Higgs boson masses of the  
 115 full combination as well as each production modes' excess and the Higgs boson coupling strength  
 116 fit of this analysis with the most recent CMS combination [17]. The couplings are SM-compatible.

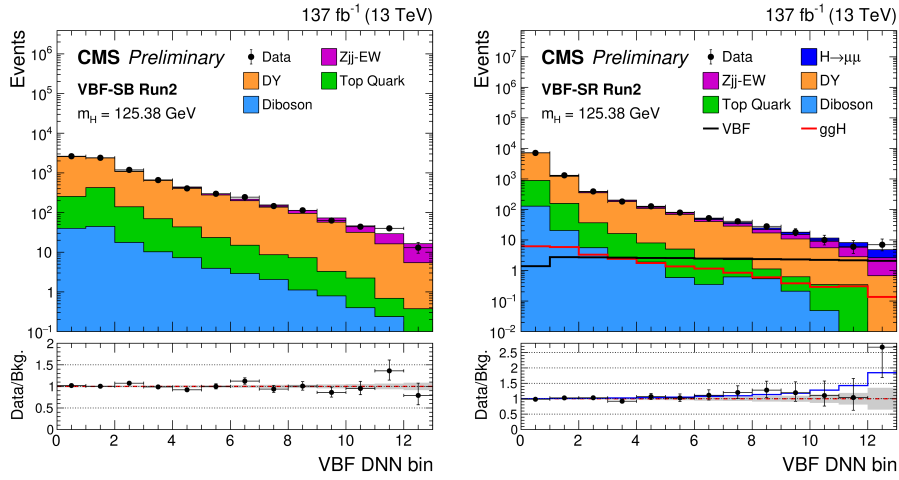


**Figure 9:** The observed DNN output distribution in the VBF sideband (left) and VBF signal (right) regions, compared to the post-fit prediction from SM processes. The lower panel shows the ratio between data and the post-fit background prediction from the signal-plus-background fit. The best-fit Higgs boson signal contribution is indicated by the blue line, and the grey band indicates the total background uncertainty [15].

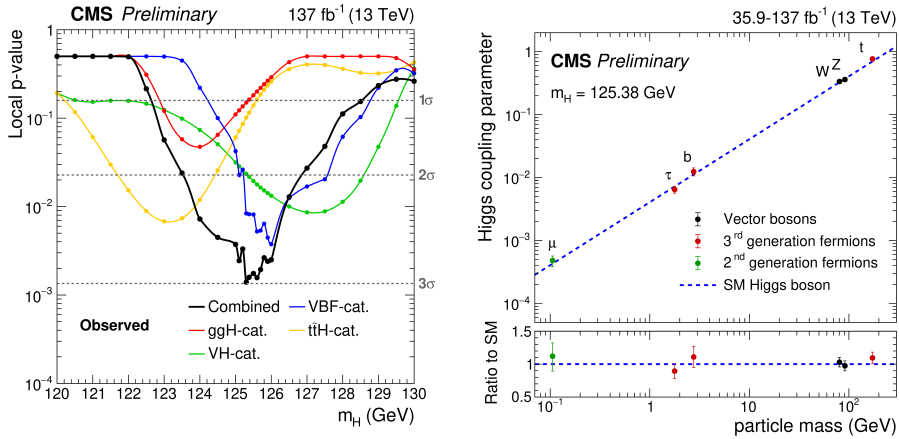


**Figure 10:** The left figure shows the p-value as a function of the hypothetical Higgs boson mass. At  $m_H = 125.38$  GeV there is a  $3.0\sigma$  excess. The slightly "bumpy" features of the VBF and combination scans are caused by low numbers of events (coming into/out of the sliding SR mass window) in the most significant DNN bins of the VBF category. On the right the fitted coupling strengths of gauge bosons, third generation fermions and the muon are shown versus their mass [15].

## 117 7. Updated combination of Higgs boson searches from ATLAS

118 ATLAS prepared an impressive combination with the most precise and fine measurements of  
 119 the Higgs boson up to this time [18]. The combination is based on the analyses of the Higgs boson  
 120 decays to photons, Z bosons, W bosons, tau leptons, bottom quarks, muons, and searches for decays  
 121 into invisible final states. Up to  $139 \text{ fb}^{-1}$  of proton–proton collision data were collected during LHC  
 122 Run 2. Combined cross section measurements are computed for ggH, VBF, VH, and ttH production  
 123 channels. The global signal strength, defined as the measured Higgs boson signal yield normalized

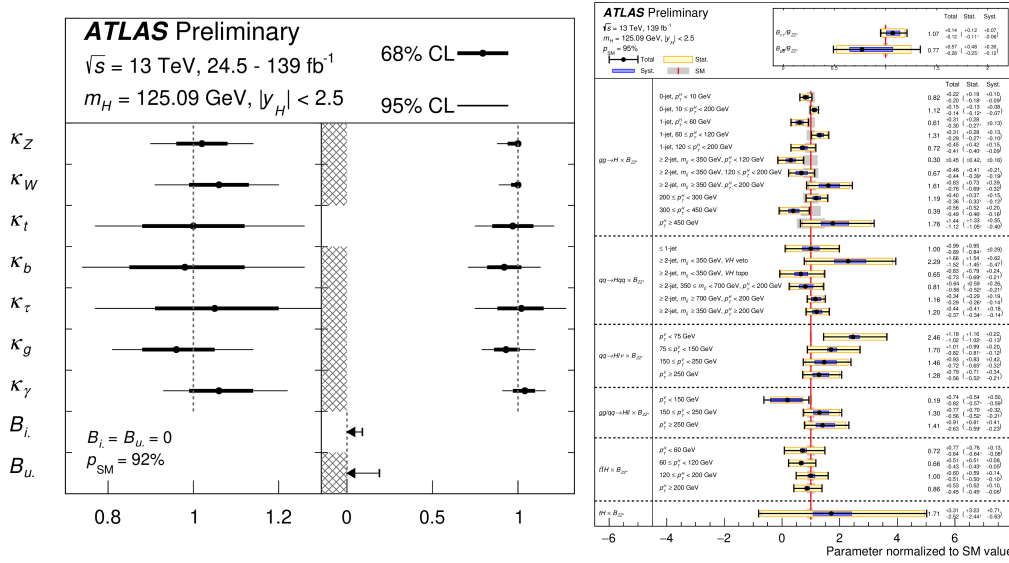


**Figure 11:** The left plot shows two  $\kappa$ -framework fits that allow couplings to the Higgs boson to float. The left fit only allows SM couplings (92% compatible with SM), and the right allows/constrains BSM couplings. The right figure shows the STXS fit with 31 measured bins (95% compatible with SM). This is the most detailed STXS measurement to date [18].

124 to its SM prediction, is determined to be  $\mu = 1.06 \pm 0.07$ , and it is note-worthy that the experimental  
 125 statistical precision ( $\pm 0.04$ ) is now smaller than the theory uncertainty ( $^{+0.05}_{-0.04}$ ).

126 There are numerous, important fits and features in this combination. The associated production  
 127 with a W boson is observed with the (expected) significance for of  $6.3\sigma$  ( $5.2\sigma$ ). Figure 11 shows the  
 128 results of three fits in two modeling frameworks. The results are interpreted in terms of modifiers  
 129 applied to the SM couplings ( $\kappa$ -framework) of the Higgs boson to other particles. That same model  
 130 is also used to set exclusion limits on parameters in two-Higgs-doublet models. Also, a 29-bin  
 131 STXS measurement is performed. No significant deviations from SM predictions are observed.

## 132 8. Summary

133 The ATLAS and CMS collaborations have completed many of the important full Run 2 Higgs  
 134 boson analyses. They are now using the discovery channels to measure detailed differential cross  
 135 sections in the STXS framework and probe anomalous couplings. Higgs boson coupling to second-  
 136 generation fermions is established with evidence of the Higgs boson decay to muons in CMS.

## 137 References

138 [1] ATLAS Collaboration. [The ATLAS experiment at the CERN LHC](#). *JINST*, 3:S08003, 2008.

139 [2] CMS Collaboration. [The CMS experiment at the CERN LHC](#). *JINST*, 3:S08004, 2008.

140 [3] CMS Collaboration. [Observation of a new boson at a mass of 125 GeV with the CMS](#)  
 141 [experiment at the LHC](#). *Phys. Lett. B*, 716:30, 2012.

- 142 [4] ATLAS Collaboration. Observation of a new particle in the search for the Standard Model  
143 Higgs boson with the ATLAS detector at the LHC. *Phys. Lett. B*, 716:1, 2012.
- 144 [5] J. Andersen et al. Les Houches 2015: Physics at TeV Colliders Standard Model Working  
145 Group Report. In *9th Les Houches Workshop on Physics at TeV Colliders*, 2016.
- 146 [6] N. Berger et al. Simplified Template Cross Sections - Stage 1.1. 2019.
- 147 [7] S. Amoroso et al. Les Houches 2019: Physics at TeV Colliders: Standard Model Working  
148 Group Report. In *11th Les Houches Workshop on Physics at TeV Colliders*, 2020.
- 149 [8] CMS Collaboration. Measurements of Higgs boson properties in the diphoton decay channel  
150 at  $\sqrt{s} = 13$  TeV, CMS-PAS-HIG-19-015. 2020.
- 151 [9] ATLAS Collaboration. Measurement of the properties of Higgs boson production at  $\sqrt{s} = 13$   
152 TeV in the  $H \rightarrow \gamma\gamma$  channel using  $139 \text{ fb}^{-1}$  of  $pp$  collision data with the ATLAS experiment,  
153 ATLAS-CONF-2020-026. 2020.
- 154 [10] ATLAS Collaboration. Observation of vector-boson-fusion production of Higgs bosons in the  
155  $H \rightarrow WW^* \rightarrow e\nu\mu\nu$  decay channel in  $pp$  collisions at  $\sqrt{s} = 13$  TeV with the ATLAS detector,  
156 ATLAS-CONF-2020-045. 2020.
- 157 [11] CMS Collaboration. Higgs boson production in association with top quarks in final states with  
158 electrons, muons, and hadronically decaying tau leptons at  $\sqrt{s} = 13$  TeV, CMS-PAS-HIG-19-  
159 008. 2020.
- 160 [12] CMS Collaboration. Constraints on anomalous Higgs boson couplings to vector bosons and  
161 fermions in production and decay in the  $H \rightarrow 4\ell$  channel, CMS-PAS-HIG-19-009. 2020.
- 162 [13] CMS Collaboration. Measurement of Higgs boson production in the decay channel with a  
163 pair of  $\tau$  leptons, CMS-PAS-HIG-19-010. 2020.
- 164 [14] CMS Collaboration. Analysis of the CP structure of the Yukawa coupling between the Higgs  
165 boson and  $\tau$  leptons in proton-proton collisions at  $\sqrt{s} = 13$  TeV, CMS-PAS-HIG-20-006.  
166 2020.
- 167 [15] CMS Collaboration. Measurement of Higgs boson decay to a pair of muons in proton-proton  
168 collisions at  $\sqrt{s}=13$  TeV, CMS-PAS-HIG-19-006. 2020.
- 169 [16] ATLAS Collaboration. A search for the dimuon decay of the Standard Model Higgs boson  
170 with the ATLAS detector. *Physics Letters B*, 812:135980, 2021.
- 171 [17] CMS Collaboration. Combined Higgs boson production and decay measurements with up to  
172  $137 \text{ fb}^{-1}$  of proton-proton collision data at  $\sqrt{s} = 13$  TeV, CMS-PAS-HIG-19-005. 2020.
- 173 [18] ATLAS Collaboration. A combination of measurements of Higgs boson production and decay  
174 using up to  $139 \text{ fb}^{-1}$  of proton-proton collision data at  $\sqrt{s} = 13$  TeV collected with the ATLAS  
175 experiment, ATLAS-CONF-2020-027. 2020.